© 2018. Published by The Company of Biologists Ltd | Development (2018) 145, dev155879. doi:10.1242/dev.155879

Tracing the destiny of mesenchymal stem cells from embryo to adult bone marrow and white adipose tissue via Pdgfrα expression

Hiroyuki Miwa*,‡ and Takumi Era‡

ABSTRACT

Mesenchymal stem cells (MSCs) are somatic stem cells that can be derived from adult bone marrow (BM) and white adipose tissue (WAT), and that display multipotency and self-renewal capacity. Although MSCs are essential for tissue formation and have already been used in clinical therapy, the origins and markers of these cells remain unknown. In this study, we first investigated the developmental process of MSCs in mouse embryos using the gene encoding platelet-derived growth factor receptor α (*Pdgfra*) as a marker. We then traced cells expressing *Pdgfra* and other genes (brachyury, *Sox1* and *Pmx1*) in various mutant mouse embryos until the adult stage. This tracing of MSC origins and destinies indicates that embryonic MSCs emerge in waves and that almost all adult BM MSCs and WAT MSCs originate from mesoderm and embryonic Pdgfrα-positive cells. Furthermore, we demonstrate that adult Pdgfrα-positive cells are involved in some pathological conditions.

KEY WORDS: Mesenchymal stem cells, Pdgfrα, Brachyury, Sox1, Pmx1 (Prrx1)

INTRODUCTION

Mesenchymal stem cells (MSCs) display self-renewal capacity, proliferation sustainability *in vitro* and the potential to differentiate into various mesenchymal cell lineages, including adipocytes, chondrocytes, and osteocytes (Prockop, 1997; Pittenger et al., 1999). MSCs are also crucial for several tissue formation processes and injury repair, including bone fracture (Grcevic et al., 2012; Mizoguchi et al., 2014; Miwa and Era, 2015). MSCs have been proposed for use in stem cell therapy because they can be derived from adult bone marrow (BM) and white adipose tissue (WAT); however, the safe and successful application of MSCs for clinical use requires clarification of their origin and the development of reliable markers for fate mapping.

Previously, we have exploited two methods for inducing mesenchymal cell lineages from embryonic stem cells (ESCs) that have also proved useful for dissecting the differentiation process *in vitro* (Wobus et al., 2002; Kawaguchi et al., 2005; Sakurai et al., 2006). The first method, which was culturing ESCs on collagen IV-coated dishes under serum-containing medium, supported the generation of mesoderm cells that can give rise to chondrocytes, osteocytes and myocytes. The other method involved treating ESCs with retinoic acid (Dani et al., 1997), thus mimicking the natural MSC differentiation pathway through neuroepithelium. This second method was demonstrated *in vivo* using a Sox1-Cre knock-in mouse line and indicated that Sox1-positive neuroepithelial cells supply the earliest wave of MSC differentiation that occurs during embryogenesis and is subsequently replaced by MSCs from other origins during postnatal development (Takashima et al., 2007). Nevertheless, our observations in these previous studies did not rule out the possibility that mesoderm could give rise to MSCs under other appropriate conditions. The current study investigates this possibility further *in vivo* using our previously generated Pdgfrα-GFPCreER^{T2} knock-in mouse line together with several other mutant mouse lines. The results define Pdgfrα as a key marker of MSC *in vivo* and show that almost all adult BM-MSC and WAT-MSC originate from mesoderm and embryonic Pdgfrα-positive cells.

RESULTS

Emergence and localization of MSC

To first investigate when MSCs emerge during mouse embryonic development, we sorted total cells from whole embryos at respective developmental stages by flow cytometry using Pdgfrα as a MSC marker, and then performed colony-forming unit-fibroblast (CFU-F) assays on the sorted cells (Fig. 1A, Fig. S1A). Colonies of CFU-F initially emerged at embryonic day 9.5 (E9.5) and were significantly increased in number between E11.5 and E14.5 (Fig. 1A). We observed no colonies in Pdgfrα-negative fractions (Fig. 1A), and E7.5 cells could not be cultured using our methods (data not shown). Correlating with the increased CFU-F colony numbers during embryo development, the percentages of Pdgfrα-positive fractions in total cells also rose from E11.5 to E13.5 (Fig. S1A). The CFU-F colony formation tendency in C57BL/6 mice was similar to that of another mouse strain, ICR (Fig. S1B,C). Furthermore, we divided whole embryos into four parts, head, trunk, limb and tail, and then sorted Pdgfrα-positive cells from each. Trunks showed a similar sorting pattern to whole embryos, whereas CFU-F colonies in heads and limbs only emerged at E13.5 (Fig. 1B). The percentages of Pdgfrα-positive fractions in all segmented parts of embryos peaked at E13.5, similar to the results for whole embryos (Fig. S1A,D). Although we examined expressions of several marker genes in Pdgfrα-positive and -negative fractions by RT-PCR, *Sca1* (*Atxn1*) and *Cd51* (*Itgav*), which have been reported as MSC markers (Morikawa et al., 2009; Pinho et al., 2013), were expressed in both fractions (Fig. S1E). These experiments suggested that embryonic MSCs emerge in waves and that Pdgfrα is a key marker of MSCs (Fig. 1A, Figs S1C and S2A); however, we could not confirm that all of CFU-F colonies were MSCs with the attendant features of self-renewal capacity and multipotency. We therefore picked up some of the CFU-F colonies derived from various stages and tissues, and established cell lines for induction into adipocytes, chondrocytes and osteocytes (Fig. S2B). CFU-F colonies from E9.5 samples showed no multipotency, whereas some was shown for

Department of Cell Modulation, Institute of Molecular Embryology and Genetics, Kumamoto University, 2-2-1 Honjo, Chuo-ku, Kumamoto 860-0811, Japan.
*Present address: Department of Pathophysiology, Tokyo University of Pharmacy and Life Sciences, 1432-1 Horinouchi, Hachioji, Tokyo 192-0392, Japan.

‡Authors for correspondence (hiroyukimiwa1026@gmail.com; tera@kumamoto-u.ac.jp)

H.M., 0000-0001-6899-7028; T.E., 0000-0003-2693-1914

Received 13 June 2017; Accepted 21 December 2017

Development (2018) 145, dev155879. doi:10.1242/dev.155879

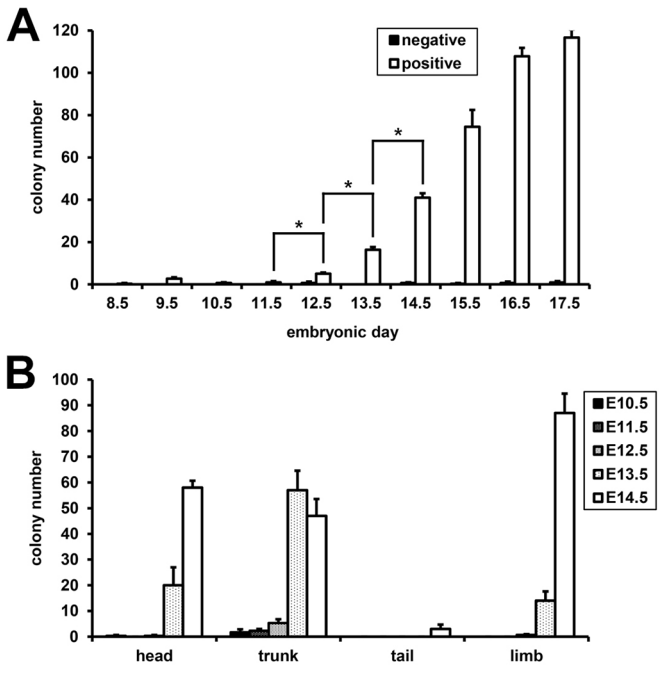

Fig. 1. Activities of Pdgfrα-positive cells as MSCs. (A) A CFU-F assay of Pdgfrα-positive and -negative cells sorted from whole embryos. Cells were plated at 1000 cells/well. Error bars represent s.e.m. n=3. *P<0.01. (B) A CFU-F assay of Pdgfrα-positive cells sorted from respective parts of embryos. Cells were plated at 3000 cells/well. Error bars represent s.e.m. n=3.

those from E11.5 and E13.5 (Table 1). Because MSCs were shown to be located in perivascular niches of both adult BM and WAT (Traktuev et al., 2008; Morikawa et al., 2009), we derived CFU-F colonies from these tissues. Almost all of the BM-derived CFU-F colonies showed multipotential differentiation, but in adult mice about half of subcutaneous WAT (sWAT)-derived CFU-F colonies did not (Table 1). These results suggest that almost all of BM-derived CFU-F colonies and half of sWAT-derived CFU-F colonies were MSCs. Moreover, adult gonadal WAT (gWAT) did not give rise to CFU-F colonies with multipotency in our experiments (Table 1). These data show that CFU-F colonies do not necessarily have proliferation capacity and multipotency in the same way as MSCs do.

Destinies of MSCs and their progenitors from embryo to adult

To trace embryonic MSCs *in vivo*, we mated a Pdgfrα-GFPCreER^{T2} knock-in mouse line generated previously (Miwa and Era, 2015) with Rosa26-Tomato mice, which can continuously express the Tomato reporter gene from various developmental stages under the control of Cre activity following treatment with 4-hydroxytamoxifen (4-OHT) (Feil et al., 1997; Madisen et al., 2010). Because pregnant mice injected with tamoxifen cannot bear pups normally, all pups were delivered by Cesarean section and nurtured by foster mothers (Samokhvalov et al., 2007; Zovein et al., 2008; Cebrian et al., 2014). We then isolated BM cells from tibiae and femora of *Pdgfrα*$^{GCE/wt}$;*Rosa26*$^{Tomato/wt}$ mice once they reached 8 weeks of age, and counted the number of Tomato-positive and -negative CFU-F colonies (Fig. 2A). Although there were no Tomato-positive colonies derived from 4-OHT-treated *Pdgfrα*$^{GCE/wt}$;*Rosa26*$^{Tomato/wt}$ BM at E6.5, almost all of CFU-F colonies from mice treated at and after E7.5 were positive for Tomato expression (Fig. 2B). Then, using *Pdgfrα*$^{GCE/wt}$;*Rosa26*$^{LacZ/wt}$ mice that continuously express the lacZ gene under Cre recombinase activity following 4-OHT treatment, X-gal staining revealed that Pdgfrα-positive cells generated at embryonic stages remained in adult BM (Fig. S3B). Indeed, E7.5 Pdgfrα-positive cells contributed to a large proportion of BM, but positive cells at and after E9.5 were limited, supporting results reported previously (Fig. S3A) (Ding et al., 2013). Moreover, almost all of CFU-F colonies derived from adult BM were continuously expressing Pdgfrα (Figs S2A and S3C). Half the dose (25 µg/g) of 4-OHT injected into pregnant mice was insufficient to recombine loxP sites by CreER^{T2} and 100 µg/g injection caused miscarriages or stillbirths in almost all cases (data not shown). *Pdgfrα*$^{GCE/wt}$;*Rosa26*$^{Tomato/wt}$ CFU-F from mice treated with vehicle at E9.5 and E10.5 did not express Tomato (Fig. S3D). Pdgfrα is expressed in the mesoderm, somite and branchial arch of the embryo (Takakura et al., 1997; Miwa and Era, 2015), which have been assumed to be where MSCs originate. Together with previous data, these findings suggest that embryonic MSCs, adult BM-MSCs and their progenitors continuously express Pdgfrα from E7.5.

To further explore the origin of MSCs in adult BM, we performed the same analyses using a Brachyury-GFPCreER^{T2} knock-in mouse line (Imuta et al., 2013; Taguchi et al., 2014) to test for a recognized mesoderm and notochord marker at between E7.5 and E9.5 (Herrmann et al., 1990). Brachyury is a transcription factor that belongs to the T-box family of molecules and is required for mesoderm formation (Bennett et al., 1972; Yanagisawa et al., 1981). We treated *Brachyury*$^{GCE/wt}$;*Rosa26*$^{Tomato/wt}$ mice with 4-OHT at E6.5, E7.5, E8.5, E9.5, E10.5 and postnatal day (P) 2, P3 and P4, and examined Tomato expression of CFU-F colonies derived from adult BM. Almost all colonies were Tomato-positive from E7.5-

Table 1. Differentiation of CFU-F colonies

	Stage or tissue	Total	Establishment	Differentiation	Multipotency
Embryo (whole)	E9.5 (ex1)	144	7	7	0
	E9.5 (ex2)	192	6	6	0
	E11.5 (ex1)	144	8	5	2
	E11.5 (ex2)	192	10	10	3
	E13.5 (ex1)	144	9	9	2
	E13.5 (ex2)	192	9	9	2
Adult (8 week)	BM	144	23	8	7
	sWAT	192	19	15	7
	gWAT (epididymal)	192	12	12	0
	gWAT (perimetric)	144	8	4	0

CFU-F colonies derived from various stages and tissues were cloned and induced.
Total, the numbers of picked up colonies; Establishment, established lines, which had proliferation capacity; Differentiation, induced lines; Multipotency, lines able to differentiate into adipocytes, chondrocytes and osteocytes, which were stained with Oil Red O, Alcian Blue and Alizarin Red S. Experiments 1 and 2 are indicated by ex1 and ex2.

Development (2018) 145, dev155879. doi:10.1242/dev.155879

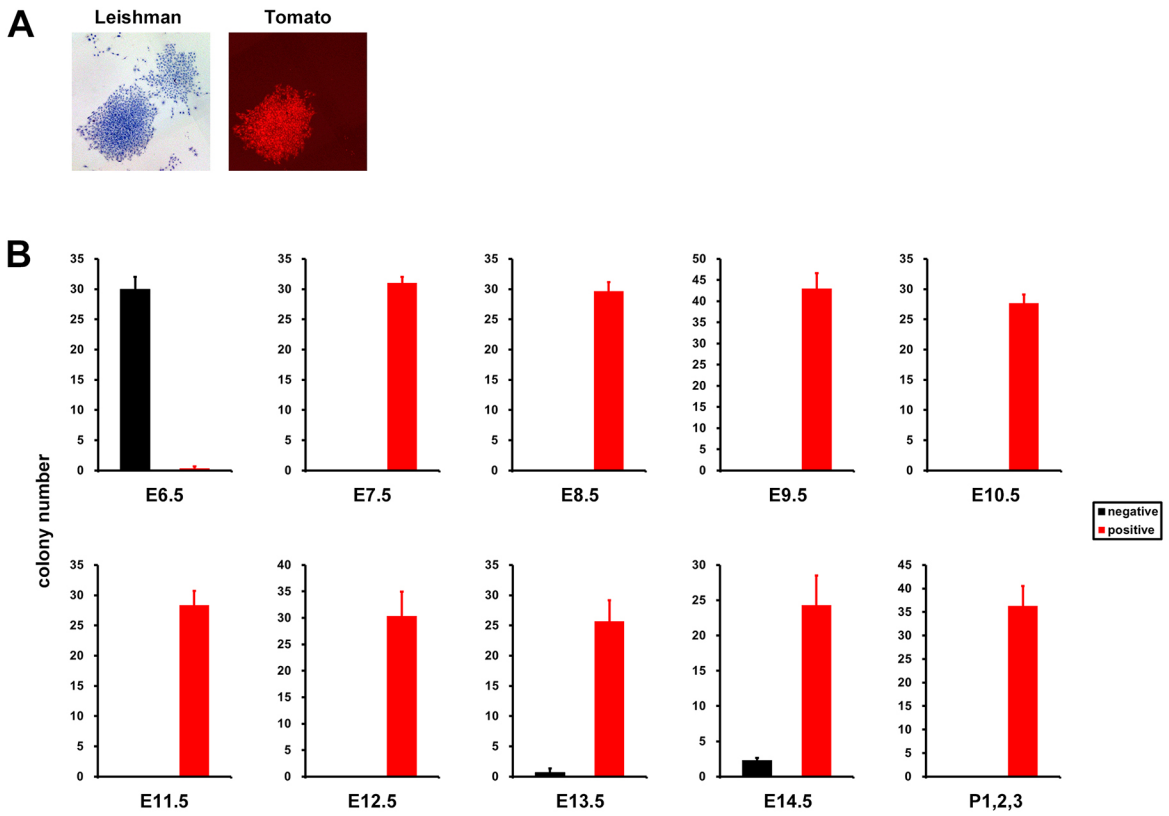

Fig. 2. Contribution of Pdgfrα-positive cells to adult BM-MSCs. (A) Images of colonies of Tomato-positive and -negative CFU-F. Colonies were stained with Leishman. (B) The colony numbers of Tomato-positive and -negative CFU-F derived from 8-week-old *Pdgfrα*$^{GCE/wt}$;*Rosa26*$^{Tomato/wt}$ BM. Treated stages are shown. Error bars represent s.e.m. *n*=3.

treated BM, but not from BM treated at any other stage during development regardless of the expression of brachyury (Fig. 3A, Figs. S1E and S4A). Additionally, adult CFU-F did not express brachyury (Fig. 3B). We further investigated whether neuroectoderm cells could contribute to adult BM-MSC using a Sox1-Cre knock-in mouse line as reported previously (Takashima et al., 2007; Yoshimura et al., 2013). Sox1 was shown to be the most specific marker for neuroepithelial cells (Fig. S1E) (Pevny et al., 1998; Aubert et al., 2003). Although we detected MSCs that originated from Sox1-positive cells in E14.5 heads (data not shown), no CFU-F colonies originating from these cells existed in adult BM (Fig. 3C). We therefore speculated that adult BM-MSCs develop from limb buds, and subsequently analyzed Pdgfrα-GFPCreER^{T2}, Brachyury-GFPCreER^{T2}, Sox1-Cre and Pmx1-Cre mutant mouse lines (Logan et al., 2002). *Pmx1* (*Prrx1*) is expressed in early limb bud mesenchyme and plays an essential role in regulating skeletal development in limbs (Fig. S1E) (Cserjesi et al., 1992; Martin et al., 1995). We found that almost all cells in limb buds originated from brachyury-positive mesoderm at E7.5, when it also expresses Pdgfrα (Fig. 3D, Fig. S4A,B). Considering the results of tracing Pmx1-positive cells (Fig. 4A), MSCs in limb buds probably develop into adult BM-MSC because limb buds and adult BM-MSC have the same origin.

Origins of adult sWAT-MSC

As for adult BM-MSC, we investigated the origins of adult sWAT-MSC using respective mutant mice. The results largely mirrored those for BM, i.e. CFU-F colonies derived from sWAT were Tomato-positive in adult *Pdgfrα*$^{GCE/wt}$;*Rosa26*$^{Tomato/wt}$ mice treated with 4-OHT at and after E7.5 (Fig. 5A), and in adult *Brachyury*$^{GCE/wt}$;*Rosa26*$^{Tomato/wt}$ mice at E7.5 and E8.5 (Fig. 5B). Negative CFU-F colonies in these assays possibly partly reflected a neuroectoderm origin (Sox1-positive cells) (Fig. 5C). Finally, Tomato-positive CFU-F colonies from Sox1 knock-in sWAT could not differentiate into three mesenchymal cell lineages (data not shown). These results suggest that almost all adult sWAT-MSC originate from mesoderm and embryonic Pdgfrα-positive cells as BM-MSCs.

Based on previous reports that Pmx1-positive cells show MSC differentiation potential (Krueger et al., 2014; Sanchez-Gurmaches et al., 2015), we examined adult BM and WAT in *Pmx1-Cre*$^{Tg/0}$;*Rosa26*$^{Tomato/wt}$ mice using Pmx1 as a marker. The majority of adult BM-MSCs were Tomato-positive, but both positive and negative CFU-F colonies were derived from adult sWAT and gWAT (Fig. 4A). Lines established from adult sWAT CFU-F could differentiate into adipocytes, chondrocytes and osteocytes regardless of expression of Tomato (Fig. 4B, Table 1). On the other hand, lines derived from adult gWAT did not give rise to adipocytes (Fig. 4C, Table 1). Our results suggest that Pmx1 is a useful marker of limb bud and adult BM-MSC, but not WAT-MSC (Figs 3D, 4A-C, Fig. S4B). In addition, almost all BM-MSCs originated from Pmx1-positive cells, whereas some sWAT-MSCs originated from Pmx1-negative cells.

Contribution of adult Pdgfrα-positive cells to pathological conditions

We next examined the role of adult Pdgfrα-positive cells under various abnormal conditions, primarily testing whether they could contribute to a bone fracture repair. Adult *Pdgfrα*$^{GCE/wt}$;

Development (2018) 145, dev155879. doi:10.1242/dev.155879

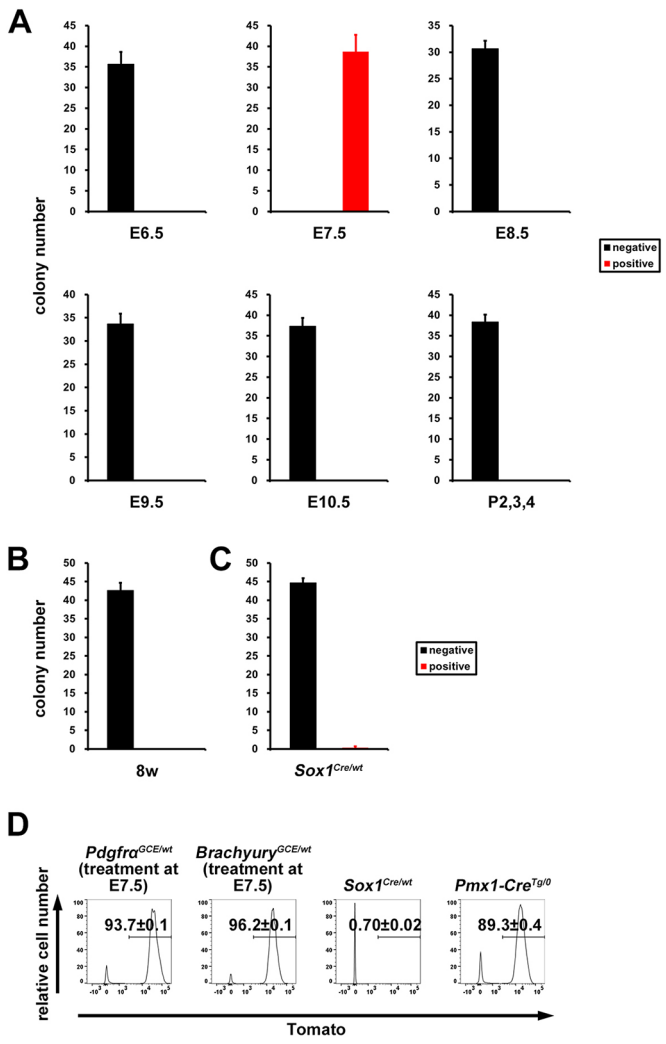

Fig. 3. Contribution of brachyury- and Sox1-positive cells to adult BM-MSCs. (A-C) The colony numbers of Tomato-positive and -negative CFU-F derived from 8-week-old *Brachyury*$^{GCE/wt}$;*Rosa26*$^{Tomato/wt}$ BM (A), from 12-week-old *Brachyury*$^{GCE/wt}$;*Rosa26*$^{Tomato/wt}$ BM treated at 8 weeks (B) and from (C) 8-week-old *Sox1*$^{Cre/wt}$;*Rosa26*$^{Tomato/wt}$ BM. Treated stages are shown in A. Error bars represent s.e.m. *n*=3. (D) Flow cytometry analysis of limb cells of various mutant mice at E13.5. The numbers represent percentages of Tomato-positive cells.

Rosa26$^{Tomato/wt}$ mice were treated with 4-OHT and their tibiae were fractured. Tomato-positive cells accumulated in the fractured sites during repair (Fig. 6A). Analyses of *Pdgfrα*$^{GCE/wt}$;*Rosa26*$^{Rainbow/wt}$ mice (Rinkevich et al., 2011) revealed Cherry-, Orange- and Cerulean-positive cells in the repaired sites with a mosaic pattern (Fig. 6B), indicating that multiple clones of MSCs contributed to fracture repair through their proliferation and differentiation.

Pdgfrα-positive cells have been associated with obesity (Lee et al., 2012); in this study, adult Pdgfrα–positive cells marked with Tomato matured into adipocytes in sWAT following a high-fat diet (Fig. 6C). Based on previous data that Pdgfrα-positive cells contribute to beige adipocytes (Lee et al., 2015), a beige marker was examined in adult *Pdgfrα*$^{GCE/wt}$;*Rosa26*$^{Tomato/wt}$ mice treated with 4-OHT. Immunostaining of harvested tissues showed that Tomato-positive cells in adult *Pdgfrα*$^{GCE/wt}$;*Rosa26*$^{Tomato/wt}$ sWAT expressed Ucp1 (Fig. 6D), which is a marker gene of beige cells (Wu et al., 2012; Kazak et al., 2015).

On the other hand, Pdgfrα-positive cells are also reported to proliferate in liver fibrosis (Campbell et al., 2005). Herein, Tomato-positive cells that also stained with Masson tricrome were detected in livers of adult *Pdgfrα*$^{GCE/wt}$;*Rosa26*$^{Tomato/wt}$ mice treated with carbon tetrachloride (Fig. S5A). In addition, skin ulcerations were repaired by Pdgfrα-positive cells (Fig. S5B), and transplanted Tomato-positive BM-MSCs were engrafted at ulcerations (Fig. S5C) (Driskell et al., 2013). In summary, our knock-in mice directly demonstrate that adult Pdgfrα-positive cells are involved in some pathological conditions and could be useful in further studies of such disorders.

DISCUSSION

In the initial part of this study, we clarified when and where MSCs emerged during embryo development. CFU-F colonies initially appeared at E9.5, but did not show multipotency until E11.5 in whole embryos. On the other hand, MSCs were markedly abundant at E13.5 in heads and limbs. To our knowledge, this study provides the first detailed determination of MSC development and indicates that embryonic MSCs emerge in waves.

Almost all of CFU-F colonies derived from adult BM were Tomato positive in *Pdgfrα*$^{GCE/wt}$;*Rosa26*$^{Tomato/wt}$ and *Brachyury*$^{GCE/wt}$;*Rosa26*$^{Tomato/wt}$ mice treated at E7.5. Colony-forming cells have a multipotency for the differentiation into three mesenchymal lineages: adipocytes, chondrocytes and osteocytes. These findings suggest, in turn, that most of BM-MSC originate from both Pdgfrα- and brachyury-positive cells at E7.5, which are mesoderm cells (Bennett et al., 1972; Yanagisawa et al., 1981; Herrmann et al., 1990; Takakura et al., 1997; Imuta et al., 2013; Miwa and Era, 2015). In contrast, some CFU-F colonies derived from adult sWAT did not express the Tomato reporter gene. Interestingly, some Tomato-positive CFU-F were detected in sWAT from *Sox1*$^{Cre/wt}$;*Rosa26*$^{Tomato/wt}$ mice, in which Sox1-positive neuroectoderm cells can be traced during development (Takashima et al., 2007; Yoshimura et al., 2013), but did not show multipotency, despite forming CFU-F-like colonies. Taken together, we can conclude that most adult BM- and sWAT-MSC originate from mesoderm, whereas the origin of some embryonic MSCs is neuroepithelium (Takashima et al., 2007). Recent studies showed that MSCs could differentiate into endoderm- and neuroectoderm-derived cells such as hepatocytes and neurons, respectively (Anjos-Afonso et al., 2004; Lee et al., 2004; Beltrami et al., 2007). Taking these findings together, MSCs should have the potential to cross germ layer boundaries.

Pdgfrα is an absolute marker of MSC in mice at least, and although MSC are currently being sorted using Pdgfrα and Sca1 from mouse BM, the latter is not always required for their isolation because MSCs exist in both Sca1-positive and -negative fractions (Morikawa et al., 2009). Furthermore, other species such as humans do not have the gene to encode Sca1 (Holmes and Stanford, 2007). Therefore, until better markers of MSCs emerge, Pdgfrα is the preferred option in mice. We confirmed that Pdgfrα-positive cells were involved in the repair of the bone fracture. Thus, Pdgfrα is one of the candidate markers for purifying functional MSC for clinical purposes, although its expression patterns in humans might be different from those in mice (Sakurai et al., 2012; Pinho et al., 2013; Li et al., 2014; Miwa and Era, 2016).

We also demonstrated that Pmx1 is a viable marker of MSC in adult BM, but not in WAT. There were no differences in morphology or proliferation between Tomato-positive and -negative MSCs derived from *Pmx1-Cre*$^{Tg/0}$;*Rosa26*$^{Tomato/wt}$ sWAT studied herein (data not shown). These data suggest that the specificity of MSC is independent of Pmx1 expression.

Development (2018) 145, dev155879. doi:10.1242/dev.155879

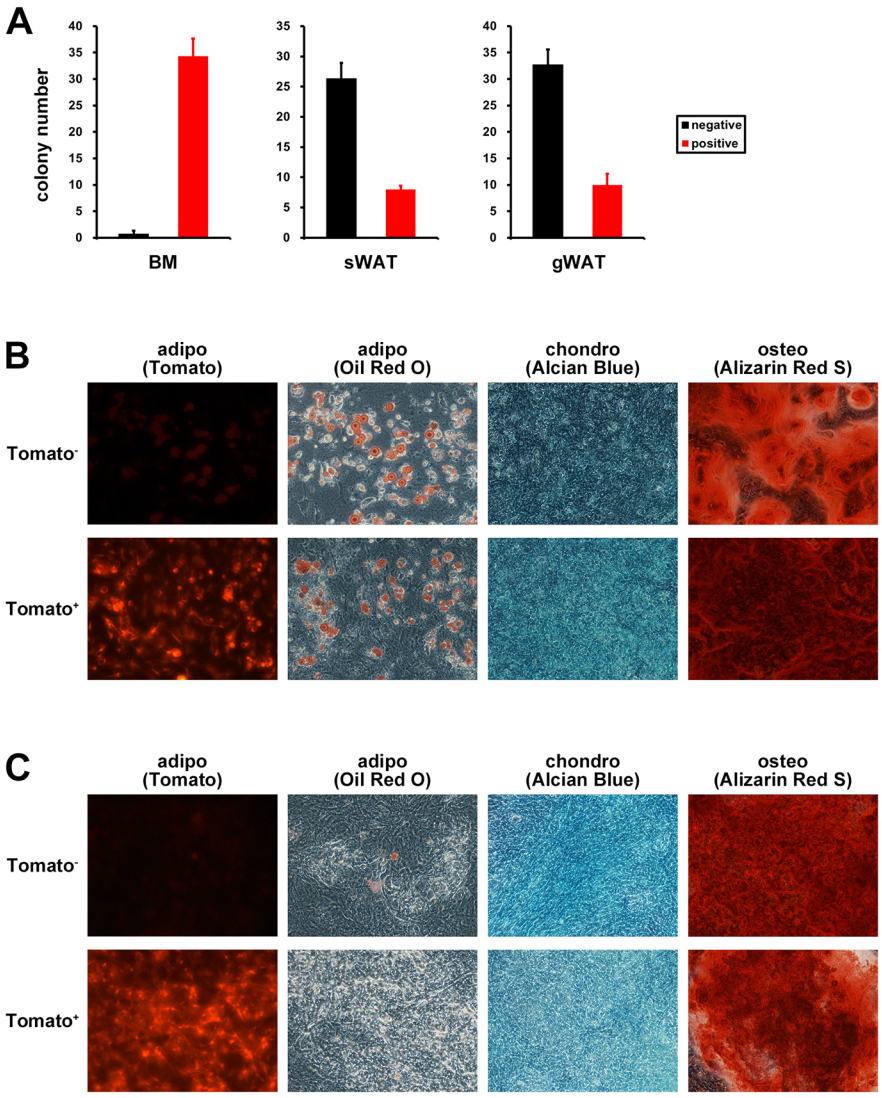

Fig. 4. Contribution of Pmx1-positive cells to adult MSCs. (A) The colony numbers of Tomato-positive and -negative CFU-F derived from 8-week-old *Pmx1-Cre*$^{Tg/0}$;*Rosa26*$^{Tomato/wt}$ BM, sWAT and gWAT. Error bars represent s.e.m. *n*=3. (B,C) Differentiation induction of sorted cells derived from 8-week-old *Pmx1-Cre*$^{Tg/0}$;*Rosa26*$^{Tomato/wt}$ sWAT (B) and *Pmx1-Cre*$^{Tg/0}$;*Rosa26*$^{Tomato/wt}$ gWAT (C) with Tomato by flow cytometry. Almost all cells derived from gWAT could not differentiate into adipocytes which were stained with Oil Red O regardless of expression of Tomato.

Alternatively, it is possible that these mutant mice non-specifically express Cre recombinase. Indeed, reporter genes were occasionally expressed wholly after mating with Pmx1-Cre transgenic mice, as reported by the mouse originators (data not shown) (Logan et al., 2002).

In studies such as this one, knock-in mice rather than transgenics should be generated when reproducing precisely the expression pattern of a target gene and activating CreER specifically (Feli et al., 1997). For example, Nestin-Cre and Wnt1-Cre transgenic mice do not always recapitulate the expression and activation of targets (Itoh et al., 2012; Lewis et al., 2013), and a Pmx1-GFPCreER^{T2} transgenic mouse line has leaky CreER activity (data not shown) (Kawanami et al., 2009). On the other hand, a knock-in Pdgfrα-GFPCreER^{T2} mouse line shows a correlation between expression of the transgene and Pdgfrα, and high-efficiency CreER function (Miwa and Era, 2015). However, depending on the design of construction, transgenes cannot occasionally be expressed substantially even in knock-in mice. It might cause some of the discrepancies between our and previous results (Ding et al., 2013). Moreover, tracing experiments from embryo to adult are rare using the CreER system due to the time and effort required: specifically, because pregnant mice administrated with tamoxifen are not able to bear pups naturally, Cesarean section and foster mothers are necessary to grow mutant mice (Samokhvalov et al., 2007; Zovein et al., 2008; Cebrian et al., 2014). The amount of tamoxifen administered to mice must be adjusted to avoid stillbirth of the pups, but still activate CreER recombination. In addition, tamoxifen does not work sufficiently on adult skin and WAT in many instances (data not shown) (Konishi et al., 2008). Therefore, although the CreER system is very powerful, a simpler and safer system is required for future studies.

We focused on mesoderm, BM and WAT in this study, although several tracings of MSC in other tissues/organs have been reported previously (Nagoshi et al., 2008; Wislet-Gendebien et al., 2012; Zhao et al., 2014; Kaukua et al., 2014; Isern et al., 2014). These studies did not investigate the derivation of MSCs in BM and WAT during the mouse development. As the *in vitro* features, including CFU-F and multipotency, initially identified and defined MSCs, the proper markers are required for detecting and tracing MSCs *in vivo*. Our results demonstrated that MSCs, which had multipotency and self-renewal capacity *in vitro*, expressed Pdgfrα at all times and could be traced using our mutant mice *in vivo*. We hope that the previous evidence is confirmed by our materials or by a similar strategy to this study in the future.

Finally, as CFU-F colonies derived from adult gWAT did not exhibit MSC multipotency in the present study, it might be

Development (2018) 145, dev155879. doi:10.1242/dev.155879

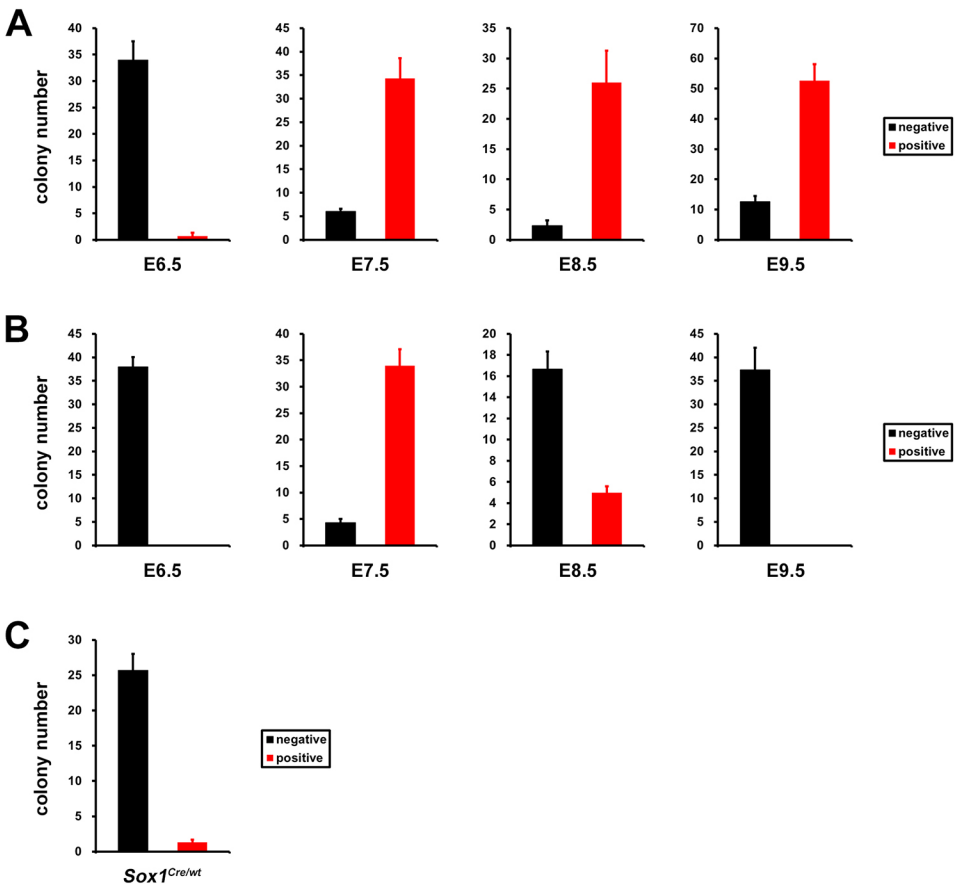

Fig. 5. Contribution of Pdgfrα-, brachyury- and Sox1-positive cells to adult sWAT-MSCs. (A-C) The colony numbers of Tomato-positive and -negative CFU-F derived from 8-week-old *Pdgfrα*$^{GCE/wt}$;*Rosa26*$^{Tomato/wt}$ sWAT (A), from 8-week-old *Brachyury*$^{GCE/wt}$;*Rosa26*$^{Tomato/wt}$ sWAT (B) and from 8-week-old *Sox1*$^{Cre/wt}$;*Rosa26*$^{Tomato/wt}$ sWAT (C). Treated stages are shown. Error bars represent s.e.m. *n*=3.

necessary to investigate the most appropriate tissues to use when MSCs are derived for clinical therapy. Unfortunately, such determination was beyond the scope of this study. Several studies have discussed the application of WAT-derived MSC for clinical therapy (Lo Furno et al., 2016). Based on our results, we recommend the careful investigation of the differences in characteristics among various adult WATs before the clinical trials (Tchkonia et al., 2005; Konishi et al., 2008).

In this study, we have demonstrated that most adult BM- and WAT-MSCs originate from mesoderm, and that this is an important finding for the safety of clinical therapy. Our results thus highlight important concepts in both developmental biology and regenerative medicine.

MATERIALS AND METHODS

Mice

The Ethics Committee of Kumamoto University approved all study protocols. The genetic background of all mice was C57BL/6. Mutant mice were genotyped using genomic DNA extracted from the tail tip and amnion in lysis buffer containing proteinase K (Wako). PCR was carried out as previously described (Soriano, 1999; Logan et al., 2002; Takashima et al., 2007; Kawanami et al., 2009; Madisen et al., 2010; Rinkevich et al., 2011; Imuta et al., 2013; Miwa and Era, 2015). All wild-type mice were purchased from CLEA Japan.

Cell culture

In order to examine differentiation potentials, we picked up single colonies of CFU-F by micropipette under a microscope and re-cultured with the MSC culture medium, which was αMEM (Gibco) containing 10% FBS and 0.1 mM 2-mercaptoethanol (Sigma) (Takashima et al., 2007; Miwa and Era, 2016).

Flow cytometry analysis

Cells were dissociated with 0.25% Trypsin-EDTA and washed with 1% bovine serum albumin-HBSS. Following staining with biotinylated anti-Pdgfrα (eBioscience) and Streptavidin APC (eBioscience), the cells were analyzed by FACS (BD Biosciences). The results were reanalyzed using FlowJo software (Tree Star).

CFU-F assay

CFU-F assays were performed as described previously (Takashima et al., 2007; Miwa and Era, 2016). Cells were set up on six-well plates at 1000-10,000 cells/well and cultured with the MSC culture medium. The culture medium was changed every 3 days. After 14 days, colonies were stained with Leishman (Merck) and counted.

Differentiation induction

Differentiation into adipocytes, chondrocytes and osteocytes was induced as described previously (Sakurai et al., 2006; Takashima et al., 2007; Miwa and Era, 2016). Briefly, cells were cultured on 24-well plates with various induction cocktails. After a certain period of time, adipocytes were stained with Oil Red O, chondrocytes with Alcian Blue and osteocytes with Alizarin Red S.

Bone fracture

Bone fracture was studied using a standard closed fracture model (Bonnarens and Einhorn, 1984). Before making bone fractures, 27-G needles were inserted into the tibia canals of anesthetized mice. Sections of bones were prepared using the Kawamoto method (Kawamoto and Shimizu, 2000).

Immunofluorescence staining

Sections were fixed with 4% paraformaldehyde in PBS and then stained with anti-Ucp1 (Abcam, ab10983, 1:500) and anti-RFP antibodies (Chromotek, 5f8, 1:1000). Alexa Fluor488- and 594-conjugated

Development (2018) 145, dev155879. doi:10.1242/dev.155879

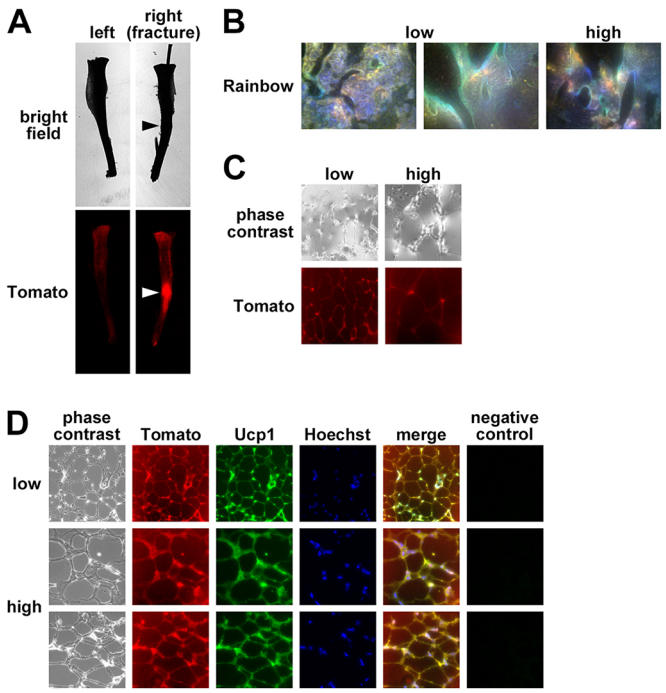

Fig. 6. Contribution of adult Pdgfrα-positive cells to pathological conditions. (A) Fractured tibia of a 12-week-old *Pdgfrα*$^{GCE/wt}$;*Rosa26*$^{Tomato/wt}$ mouse. The mouse was treated with 4-OHT at 8 weeks and operated on at 9 weeks. Arrowheads indicate fracture sites. (B) Fractured tibia of a 12-week-old *Pdgfrα*$^{GCE/wt}$;*Rosa26*$^{Rainbow/wt}$ mouse. The mouse was treated with 4-OHT at 8 weeks and operated on at 9 weeks. 'Low' and 'high' refer to magnification. (C) sWAT of a 12-week-old *Pdgfrα*$^{GCE/wt}$;*Rosa26*$^{Tomato/wt}$ mouse. The mouse was treated with 4-OHT at 8 weeks and was fed with a high-fat diet from 9 weeks. 'Low' and 'high' refer to magnification. (D) Immunofluorescence staining of *Pdgfrα*$^{GCE/wt}$;*Rosa26*$^{Tomato/wt}$ sWAT with Ucp1. The mouse was treated with 4-OHT at 8 weeks and housed at 4°C for a further 2 days. A species- and isotype-matched polyclonal antibody was used as a negative control. 'Low' and 'high' refer to magnification. Ucp1 is the marker of beige cells and not usually expressed in WAT.

secondary antibodies (Invitrogen, A-11008, A-11007, 1:50) were used for primary antibody detection.

Treatment with 4-OHT

The day of vaginal plug formation was recorded as E0.5. 4-OHT (Sigma) was dissolved in ethanol at a concentration of 100 mg/ml and then diluted in corn oil (Sigma) to a concentration of 10 mg/ml. Pregnant mice were injected intraperitoneally with 4-OHT at 50 µg/g body weight. Adult mice were injected intraperitoneally with 4-OHT once a day or fed with a powdered diet containing 500 µg/g of tamoxifen (Sigma) for 5 days.

RT-PCR

Total RNA was purified with Sepasol Super G reagent (Nacalai Tesque) and transcribed to DNA using PrimeScript (Takara). Quantitative PCR was performed using THUNDERBIRD SYBR qPCR Mix (Toyobo) as described previously (Kitagawa et al., 2012). The data were analyzed with PikoReal 96 Real-Time PCR System (Thermo Scientific) and normalized to β-actin and *Gapdh*. The sequences of primers are listed in Table S1.

X-Gal staining

To detect expression of *LacZ*, sections were fixed and stained as described previously (Houzelstein et al., 1997). The fixative solution used was 2% formaldehyde and 0.2% glutaraldehyde in PBS. The staining solution used was 1 mg/ml X-Gal (Wako), 5 mM potassium ferricyanide, 5 mM potassium ferrocyanide, 2 mM $MgCI_2$, 0.01% sodium deoxycholate and 0.02% Nonidet P-40 (NP-40) in PBS.

Liver fibrosis

Liver fibrosis was induced by repeated intraperitoneal carbon tetrachloride (Wako) injections into mice (eight times per day every 3 days). Carbon tetrachloride was dissolved in an equal volume of corn oil (Sigma) and injected at a dose of 1 µl/g body weight. Sections stained with Masson trichrome were examined with light microscopy (Hotta et al., 2008).

Skin ulceration

Mice were anesthetized with an intraperitoneal injection of ketamine and xylazine. The dorsal surface was shaved and a disposable 0.6 cm diameter skin-punch biopsy tool was used to create a full-thickness excision wound that extended to the fascia, as described elsewhere (Goto et al., 2006). For MSC transplantation, we suspended 100,000 MSCs in 160 µl PBS and subcutaneously injected them around ulcerations.

Statistical analysis

Data are expressed as the mean±s.e.m. All experiments were independently repeated at least three times. The statistical significance of differences in mean values was assessed using Student's *t*-test.

Acknowledgements

We thank Dr Hiroshi Sasaki for kindly providing Brachyury-GFPCreER^{T2} mice and Dr Hiroo Ueno for kindly providing Rosa26-Rainbow mice. We also thank the Center for Animal Resources and Development (CARD) of Kumamoto University for generating and housing the mutant and control mice.

Competing interests

The authors declare no competing or financial interests.

Author contributions

Conceptualization: H.M., T.E.; Methodology: H.M., T.E.; Validation: H.M., T.E.; Formal analysis: H.M., T.E.; Investigation: H.M., T.E.; Resources: H.M., T.E.; Data curation: H.M., T.E.; Writing - original draft: H.M.; Writing - review & editing: T.E.; Visualization: H.M., T.E.; Supervision: H.M., T.E.; Project administration: H.M., T.E.; Funding acquisition: T.E.

Funding

This study was supported, in part, by grants from the Ministry of Health, Labor and Welfare, the Japan Agency for Medical Research and Development (AMED), the Core Research for Evolutional Science and Technology (CREST) and the Japan Science and Technology Agency (JST).

Supplementary information

Supplementary information available online at
http://dev.biologists.org/lookup/doi/10.1242/dev.155879.supplemental

References

Anjos-Afonso, F., Siapati, E. K. and Bonnet, D. (2004). In vivo contribution of murine mesenchymal stem cells into multiple cell-types under minimal damage conditions. *J. Cell Sci.* **117**, 5655-5664.

Aubert, J., Stavridis, M. P., Tweedie, S., O'Reilly, M., Vierlinger, K., Li, M., Ghazal, P., Pratt, T., Mason, J. O., Roy, D. et al. (2003). Screening for mammalian neural genes via fluorescence-activated cell sorter purification of neural precursors from Sox1-gfp knock-in mice. *Proc. Natl. Acad. Sci. USA* **100**Suppl. 1, 11836-11841.

Beltrami, A. P., Cesselli, D., Bergamin, N., Marcon, P., Rigo, S., Puppato, E., D'Aurizio, F., Verardo, R., Piazza, S., Pignatelli, A. et al. (2007). Multipotent cells can be generated in vitro from several adult human organs (heart, liver, and bone marrow). *Blood* **110**, 3438-3446.

Bennett, D., Goldberg, E., Dunn, L. C. and Boyse, E. A. (1972). Serological detection of a cell-surface antigen specified by the T (brachyury) mutant gene in the house mouse. *Proc. Natl. Acad. Sci. USA* **69**, 2076-2080.

Bonnarens, F. and Einhorn, T. A. (1984). Production of a standard closed fracture in laboratory animal bone. *J. Orthop. Res.* **2**, 97-101.

Campbell, J. S., Hughes, S. D., Gilbertson, D. G., Palmer, T. E., Holdren, M. S., Haran, A. C., Odell, M. M., Bauer, R. L., Ren, H.-P., Haugen, H. S. et al. (2005). Platelet-derived growth factor C induces liver fibrosis, steatosis, and hepatocellular carcinoma. *Proc. Natl. Acad. Sci. USA* **102**, 3389-3394.

Cebrian, C., Asai, N., D'Agati, V. and Costantini, F. (2014). The number of fetal nephron progenitor cells limits ureteric branching and adult nephron endowment. *Cell Rep.* **7**, 127-137.

Cserjesi, P., Lilly, B., Bryson, L., Wang, Y., Sassoon, D. A. and Olson, E. N. (1992). Mhox: a mesodermally restricted homeodomain protein that binds an

essential site in the muscle creative kinase enhancer. *Development* **115**, 1087-1101.
Dani, C., Smith, A. G., Dessolin, S., Leroy, P., Staccini, L., Villageois, P., Darimont, C. and Ailhaud, G. (1997). Differentiation of embryonic stem cells into adipocytes in vitro. *J. Cell Sci.* **110**, 1279-1285.
Ding, G., Tanaka, Y., Hayashi, M., Nishikawa, S.-I. and Kataoka, H. (2013). PDGF receptor alpha+ mesoderm contributes to endothelial and hematopoietic cells in mice. *Dev. Dyn.* **242**, 254-268.
Driskell, R. R., Lichtenberger, B. M., Hoste, E., Kretzschmar, K., Simons, B. D., Charalambous, M., Ferron, S. R., Herault, Y., Pavlovic, G., Ferguson-Smith, A. C. et al. (2013). Distinct fibroblast lineages determine dermal architecture in skin development and repair. *Nature* **504**, 277-281.
Feil, R., Wagner, J., Metzger, D. and Chambon, P. (1997). Regulation of Cre recombinase activity by mutated estrogen receptor ligand-binding domains. *Biochem. Biophys. Res. Commun.* **237**, 752-757.
Goto, M., Sumiyoshi, H., Sakai, T., Fässler, R., Ohashi, S., Adachi, E., Yoshioka, H. and Fujiwara, S. (2006). Elimination of epiplakin by gene targeting results in acceleration of keratinocyte migration in mice. *Mol. Cell. Biol.* **26**, 548-558.
Grcevic, D., Pejda, S., Matthews, B. G., Repic, D., Wang, L., Li, H., Kronenberg, M. S., Jiang, X., Maye, P., Adams, D. J. et al. (2012). In vivo fate mapping identifies mesenchymal progenitor cells. *Stem Cells* **30**, 187-196.
Herrmann, B. G., Labeit, S., Poustka, A., King, T. R. and Lehrach, H. (1990). Cloning of the T gene required in mesoderm formation in the mouse. *Nature* **343**, 617-622.
Holmes, C. and Stanford, W. L. (2007). Concise review: stem cell antigen-1: expression, function, and enigma. *Stem Cells* **25**, 1339-1347.
Hotta, Y., Sasaki, S., Konishi, M., Kinoshita, H., Kuwahara, K., Nakao, K. and Itoh, N. (2008). Fgf16 is required for cardiomyocyte proliferation in the mouse embryonic heart. *Dev. Dyn.* **237**, 2947-2954.
Houzelstein, D., Cohen, A., Buckingham, M. E. and Robert, B. (1997). Insertional mutation of the mouse Msx1 homeobox gene by an nlacZ reporter gene. *Mech. Dev.* **65**, 123-133.
Imuta, Y., Kiyonari, H., Jang, C.-W., Behringer, R. R. and Sasaki, H. (2013). Generation of knock-in mice that express nuclear enhanced green fluorescent protein and tamoxifen-inducible Cre recombinase in the notochord from Foxa2 and T loci. *Genesis* **51**, 210-218.
Isern, J., García-García, A., Martín, A. M., Arranz, L., Martín-Pérez, D., Torroja, C., Sánchez-Cabo, F. and Méndez-Ferrer, S. (2014). The neural crest is a source of mesenchymal stem cells with specialized hematopoietic stem cell niche function. *Elife* **3**, e03696.
Itoh, M., Tahimic, C. G., Ide, S., Otsuki, A., Sasaoka, T., Noguchi, S., Oshimura, M., Goto, Y. and Kurimasa, A. (2012). Methyl CpG-binding protein isoform MeCP2_e2 is dispensable for Rett syndrome phenotypes but essential for embryo viability and placenta development. *J. Biol. Chem.* **287**, 13859-13867.
Kaukua, N., Shahidi, M. K., Konstantinidou, C., Dyachuk, V., Kaucka, M., Furlan, A., An, Z., Wang, L., Hultman, I., Ahrlund-Richter, L. et al. (2014). Glial origin of mesenchymal stem cells in a tooth model system. *Nature* **513**, 551-554.
Kawaguchi, J., Mee, P. J. and Smith, A. G. (2005). Osteogenic and chondrogenic differentiation of embryonic stem cells in response to specific growth factors. *Bone* **36**, 758-769.
Kawamoto, T. and Shimizu, M. (2000). A method for preparing 2- to 50-micron-thick fresh-frozen sections of large samples and undecalcified hard tissues. *Histochem. Cell Biol.* **113**, 331-339.
Kawanami, A., Matsushita, T., Chan, Y. Y. and Murakami, S. (2009). Mice expressing GFP and CreER in osteochondro progenitor cells in the periosteum. *Biochem. Biophys. Res. Commun.* **386**, 477-482.
Kazak, L., Chouchani, E. T., Jedrychowski, M. P., Erickson, B. K., Shinoda, K., Cohen, P., Vetrivelan, R., Lu, G. Z., Laznik-Bogoslavski, D., Hasenfuss, S. C. et al. (2015). A creatine-driven substrate cycle enhances energy expenditure and thermogenesis in beige fat. *Cell* **163**, 643-655.
Kitagawa, M., Takebe, A., Ono, Y., Imai, T., Nakao, K., Nishikawa, S. and Era, T. (2012). Phf14, a novel regulator of mesenchyme growth via platelet-derived growth factor (PDGF) receptor-α. *J. Biol. Chem.* **287**, 27983-27996.
Konishi, M., Nakamura, H., Miwa, H., Chambon, P., Ornitz, D. M. and Itoh, N. (2008). Role of Fgf receptor 2c in adipocyte hypertrophy in mesenteric white adipose tissue. *Mol. Cell. Endocrinol.* **287**, 13-19.
Krueger, K. C., Costa, M. J., Du, H. and Feldman, B. J. (2014). Characterization of Cre recombinase activity for in vivo targeting of adipocyte precursor cells. *Stem Cell Reports* **3**, 1147-1158.
Lee, K.-D., Kuo, T. K., Whang-Peng, J., Chung, Y.-F., Lin, C.-T., Chou, S.-H., Chen, J.-R., Chen, Y.-P. and Lee, O. K. (2004). In vitro hepatic differentiation of human mesenchymal stem cells. *Hepatology* **40**, 1275-1284.
Lee, Y.-H., Petkova, A. P., Mottillo, E. P. and Granneman, J. G. (2012). In vivo identification of bipotential adipocyte progenitors recruited by b3-adrenoceptor activation and high-fat feeding. *Cell Metab.* **15**, 480-491.
Lee, M.-W., Odegaard, J. I., Mukundan, L., Qiu, Y., Molofsky, A. B., Nussbaum, J. C., Yun, K., Locksley, R. M. and Chawla, A. (2015). Activated type 2 innate lymphoid cells regulate beige fat biogenesis. *Cell* **160**, 74-87.
Lewis, A. E., Vasudevan, H. N., O'Neill, A. K., Soriano, P. and Bush, J. O. (2013). The widely used Wnt1-Cre transgene causes developmental phenotypes by ectopic activation of Wnt signaling. *Dev. Biol.* **379**, 229-234.
Li, H., Ghazanfari, R., Zacharaki, D., Ditzel, N., Isern, J., Ekblom, M., Méndez-Ferrer, S., Kassem, M. and Scheding, S. (2014). Low/negative expression of PDGFR-α identifies the candidate primary mesenchymal stromal cells in adult human bone marrow. *Stem Cell Rep.* **3**, 965-974.
Lo Furno, D., Mannino, G., Cardile, V., Parenti, R. and Giuffrida, R. (2016). Potential Therapeutic Applications of Adipose-Derived Mesenchymal Stem Cells. *Stem Cells Dev.* **25**, 1615-1628.
Logan, M., Martin, J. F., Nagy, A., Lobe, C., Olson, E. N. and Tabin, C. J. (2002). Expression of Cre Recombinase in the developing mouse limb bud driven by a Prxl enhancer. *Genesis* **33**, 77-80.
Madisen, L., Zwingman, T. A., Sunkin, S. M., Oh, S. W., Zariwala, H. A., Gu, H., Ng, L. L., Palmiter, R. D., Hawrylycz, M. J., Jones, A. R. et al. (2010). A robust and high-throughput Cre reporting and characterization system for the whole mouse brain. *Nat. Neurosci.* **13**, 133-140.
Martin, J. F., Bradley, A. and Olson, E. N. (1995). The paired-like homeobox gene MHox is required for early events of skeletogenesis in multiple lineages. *Genes Dev.* **9**, 1237-1249.
Miwa, H. and Era, T. (2015). Generation and characterization of PDGFRα-GFPCreERT2 knock-in mouse line. *Genesis* **53**, 329-336.
Miwa, H. and Era, T. (2016). Mesoderm Differentiation from hiPS Cells. *Methods Mol. Biol.* **1357**, 403-413.
Mizoguchi, T., Pinho, S., Ahmed, J., Kunisaki, Y., Hanoun, M., Mendelson, A., Ono, N., Kronenberg, H. M. and Frenette, P. S. (2014). Osterix marks distinct waves of primitive and definitive stromal progenitors during bone marrow development. *Dev. Cell* **29**, 340-349.
Morikawa, S., Mabuchi, Y., Kubota, Y., Nagai, Y., Niibe, K., Hiratsu, E., Suzuki, S., Miyauchi-Hara, C., Nagoshi, N., Sunabori, T. et al. (2009). Prospective identification, isolation, and systemic transplantation of multipotent mesenchymal stem cells in murine bone marrow. *J. Exp. Med.* **206**, 2483-2496.
Nagoshi, N., Shibata, S., Kubota, Y., Nakamura, M., Nagai, Y., Satoh, E., Morikawa, S., Okada, Y., Mabuchi, Y., Katoh, H. et al. (2008). Ontogeny and multipotency of neural crest-derived stem cells in mouse bone marrow, dorsal root ganglia, and whisker pad. *Cell Stem Cell* **2**, 392-403.
Pevny, L. H., Sockanathan, S., Placzek, M. and Lovell-Badge, R. (1998). A role for SOX1 in neural determination. *Development* **125**, 1967-1978.
Pinho, S., Lacombe, J., Hanoun, M., Mizoguchi, T., Bruns, I., Kunisaki, Y. and Frenette, P. S. (2013). PDGFRα and CD51 mark human nestin+ sphere-forming mesenchymal stem cells capable of hematopoietic progenitor cell expansion. *J. Exp. Med.* **210**, 1351-1367.
Pittenger, M. F., Mackay, A. M., Beck, S. C., Jaiswal, R. K., Douglas, R., Mosca, J. D., Moorman, M. A., Simonetti, D. W., Craig, S. and Marshak, D. R. (1999). Multilineage potential of adult human mesenchymal stem cells. *Science* **284**, 143-147.
Prockop, D. J. (1997). Marrow stromal cells as stem cells for nonhematopoietic tissues. *Science* **276**, 71-74.
Rinkevich, Y., Lindau, P., Ueno, H., Longaker, M. T. and Weissman, I. L. (2011). Germ-layer and lineage-restricted stem/progenitors regenerate the mouse digit tip. *Nature* **476**, 409-413.
Sakurai, H., Era, T., Jakt, L. M., Okada, M., Nakai, S., Nishikawa, S. and Nishikawa, S.-I. (2006). In vitro modeling of paraxial and lateral mesoderm differentiation reveals early reversibility. *Stem Cells* **24**, 575-586.
Sakurai, H., Sakaguchi, Y., Shoji, E., Nishino, T., Maki, I., Sakai, H., Hanaoka, K., Kakizuka, A. and Sehara-Fujisawa, A. (2012). In vitro modeling of paraxial mesodermal progenitors derived from induced pluripotent stem cells. *PLoS One* **7**, e47078.
Samokhvalov, I. M., Samokhvalova, N. I. and Nishikawa, S. (2007). Cell tracing shows the contribution of the yolk sac to adult haematopoiesis. *Nature* **446**, 1056-1061.
Sanchez-Gurmaches, J., Hsiao, W.-Y. and Guertin, D. A. (2015). Highly selective in vivo labeling of subcutaneous white adipocyte precursors with Prx1-Cre. *Stem Cell Rep.* **4**, 541-550.
Soriano, P. (1999). Generalized lacZ expression with the ROSA26 Cre reporter strain. *Nat. Genet.* **21**, 70-71.
Taguchi, A., Kaku, Y., Ohmori, T., Sharmin, S., Ogawa, M., Sasaki, H. and Nishinakamura, R. (2014). Redefining the in vivo origin of metanephric nephron progenitors enables generation of complex kidney structures from pluripotent stem cells. *Cell Stem Cell* **14**, 53-67.
Takakura, N., Yoshida, H., Ogura, Y., Kataoka, H., Nishikawa, S. and Nishikawa, S. (1997). PDGFR alpha expression during mouse embryogenesis: immunolocalization analyzed by whole-mount immunohistostaining using the monoclonal anti-mouse PDGFR alpha antibody APA5. *J. Histochem. Cytochem.* **45**, 883-893.
Takashima, Y., Era, T., Nakao, K., Kondo, S., Kasuga, M., Smith, A. G. and Nishikawa, S.-I. (2007). Neuroepithelial cells supply an initial transient wave of MSC differentiation. *Cell* **129**, 1377-1388.
Tchkonia, T., Tchoukalova, Y. D., Giorgadze, N., Pirtskhalava, T., Karagiannides, I., Forse, R. A., Koo, A., Stevenson, M., Chinnappan, D.,

Cartwright, A. et al. (2005). Abundance of two human preadipocyte subtypes with distinct capacities for replication, adipogenesis, and apoptosis varies among fat depots. *Am. J. Physiol. -Endocrinol. Metab.* **288**, E267-E277.

Traktuev, D. O., Merfeld-Clauss, S., Li, J., Kolonin, M., Arap, W., Pasqualini, R., Johnstone, B. H. and March, K. L. (2008). A population of multipotent CD34-positive adipose stromal cells share pericyte and mesenchymal surface markers, reside in a periendothelial location, and stabilize endothelial networks. *Circ. Res.* **102**, 77-85.

Wislet-Gendebien, S., Laudet, E., Neirinckx, V., Alix, P., Leprince, P., Glejzer, A., Poulet, C., Hennuy, B., Sommer, L., Shakhova, O. et al. (2012). Mesenchymal stem cells and neural crest stem cells from adult bone marrow: characterization of their surprising similarities and differences. *Cell. Mol. Life Sci.* **69**, 2593-2608.

Wobus, A. M., Guan, K., Yang, H. T. and Boheler, K. R. (2002). Embryonic stem cells as a model to study cardiac, skeletal muscle, and vascular smooth muscle cell differentiation. *Methods Mol. Biol.* **185**, 127-156.

Wu, J., Boström, P., Sparks, L. M., Ye, L., Choi, J. H., Giang, A. H., Khandekar, M., Virtanen, K. A., Nuutila, P., Schaart, G. et al. (2012). Beige adipocytes are a distinct type of thermogenic fat cell in mouse and human. *Cell* **150**, 366-376.

Yanagisawa, K. O., Fujimoto, H. and Urushihara, H. (1981). Effects of the brachyury (T) mutation on morphogenetic movement in the mouse embryo. *Dev. Biol.* **87**, 242-248.

Yoshimura, N., Motohashi, T., Aoki, H., Tezuka, K., Watanabe, N., Wakaoka, T., Era, T. and Kunisada, T. (2013). Dual origin of melanocytes defined by Sox1 expression and their region-specific distribution in mammalian skin. *Dev. Growth Differ.* **55**, 270-281.

Zhao, H., Feng, J., Seidel, K., Shi, S., Klein, O., Sharpe, P. and Chai, Y. (2014). Secretion of shh by a neurovascular bundle niche supports mesenchymal stem cell homeostasis in the adult mouse incisor. *Cell Stem Cell* **14**, 160-173.

Zovein, A. C., Hofmann, J. J., Lynch, M., French, W. J., Turlo, K. A., Yang, Y., Becker, M. S., Zanetta, L., Dejana, E., Gasson, J. C. et al. (2008). Fate tracing reveals the endothelial origin of hematopoietic stem cells. *Cell Stem Cell* **3**, 625-636.

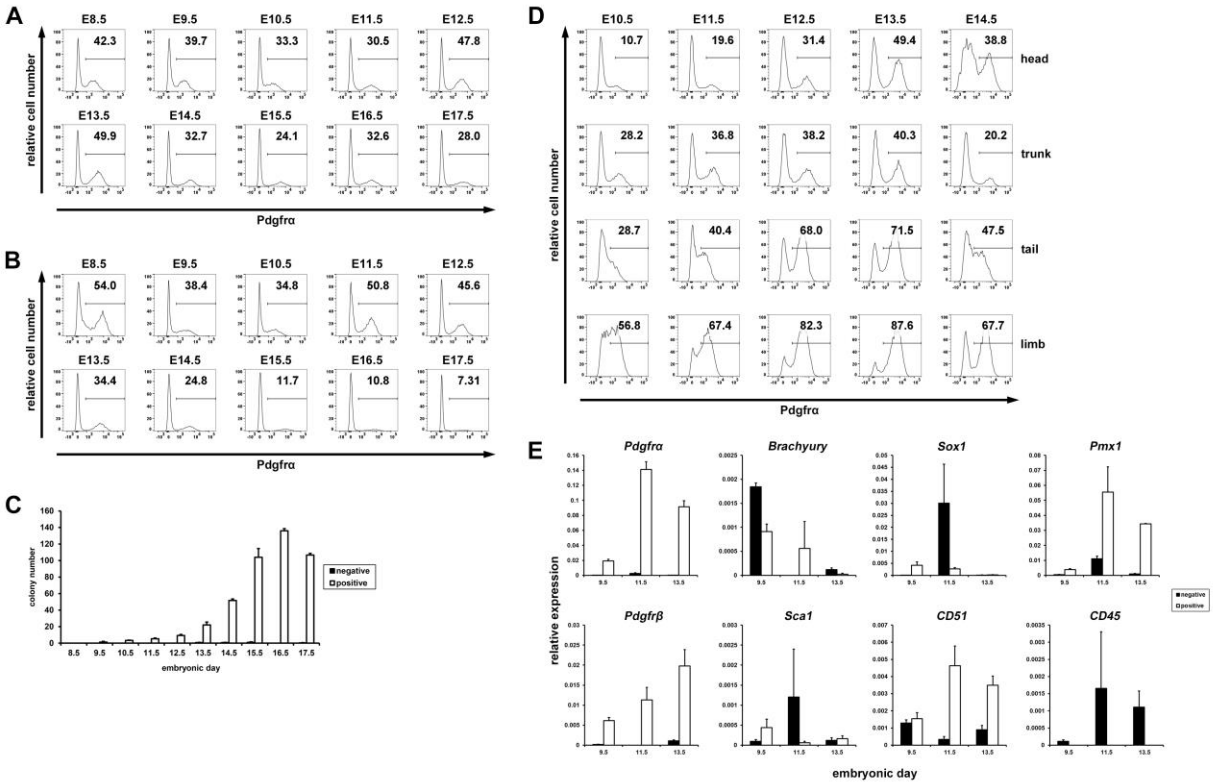

Fig. S1.

(A) Sorting whole embryos with Pdgfrα by flow cytometer. The numbers represent percentages of Pdgfrα-positive cells.

(B) Sorting ICR whole embryos with Pdgfrα by flow cytometer. The numbers represent percentages of Pdgfrα-positive cells.

(C) CFU-F assay of sorted cells in B. Cells were plated at 1,000 cells/well. Error bars represent SEM. n = 3.

(D) Sorting respective parts of embryos with Pdgfrα by flow cytometer. The numbers represent percentages of Pdgfrα-positive cells.

(E) Expression of marker genes in sorted cells in A. Error bars represent

SEM. n = 3-5.

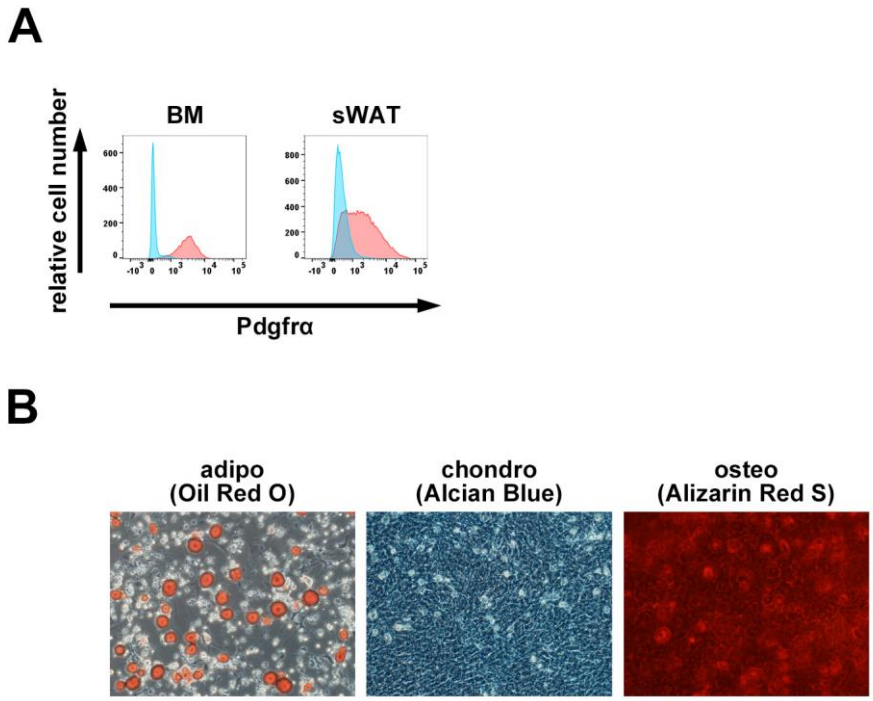

Fig. S2.

(A) Flow cytometry analysis of CFU-F derived from 8w BM and sWAT. Red and blue lines indicate stained and unstained cells, respectively.

(B) Differentiation induction of CFU-F derived from 8w BM into adipocytes, chondrocytes, and osteocytes.

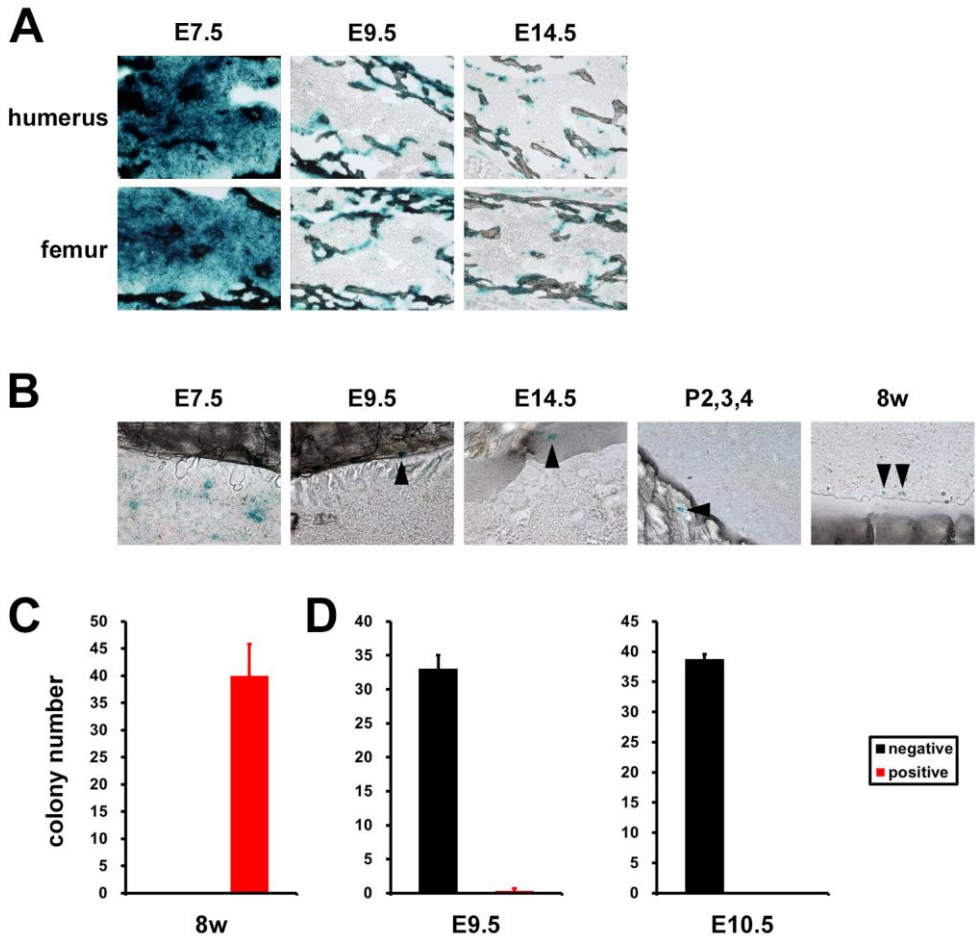

Fig. S3.

(A) E20.5 *Pdgfra*$^{GCE/wt}$;*Rosa26*$^{LacZ/wt}$ BM. Treated stages are shown.

(B) 12w *Pdgfra*$^{GCE/wt}$;*Rosa26*$^{LacZ/wt}$ BM. Treated stages are shown. Arrowheads indicate LacZ-positive cells.

(C) The colony numbers of Tomato-positive and -negative CFU-F derived from 12w *Pdgfra*$^{GCE/wt}$;*Rosa26*$^{Tomato/wt}$ BM treated at 8w. Error bars represent SEM. n = 3.

(D) The colony numbers of Tomato-positive and -negative CFU-F derived from 8w *Pdgfra*$^{GCE/wt}$;*Rosa26*$^{Tomato/wt}$ BM treated with vehicle at E9.5 and 10.5. Error bars represent SEM. n = 3.

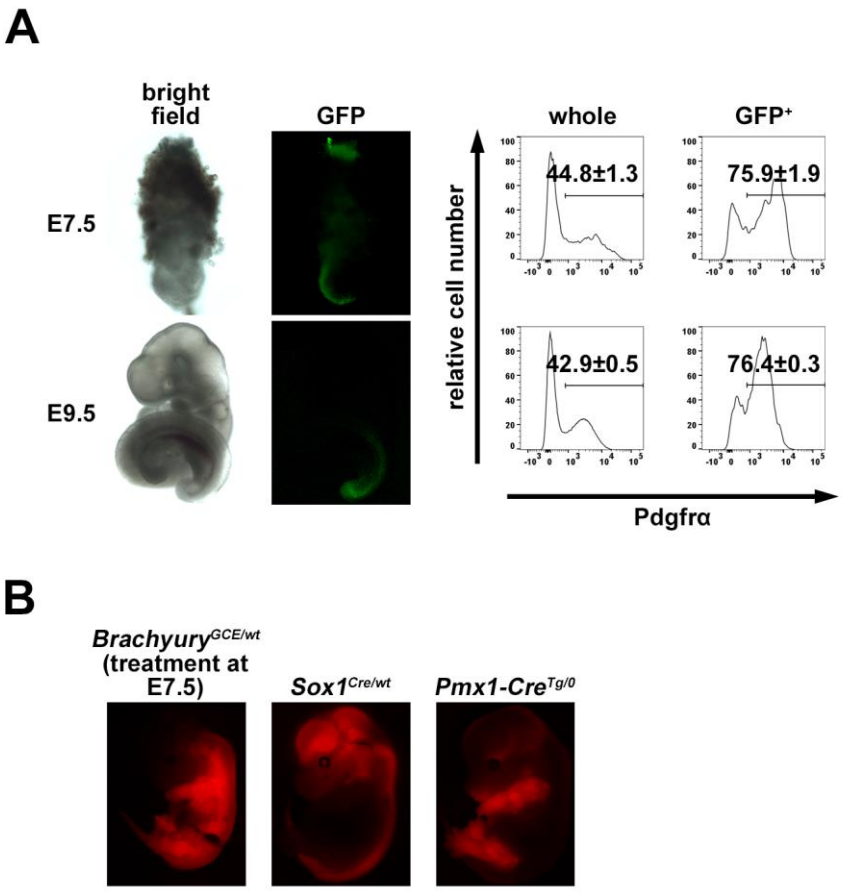

Fig. S4.

(A) Flow cytometry analysis of E7.5 and 9.5 *Brachyury*$^{GCE/wt}$ embryos. The numbers represent percentages of Pdgfrα-positive cells.

(B) E13.5 *Brachyury*$^{GCE/wt}$;*Rosa26*$^{Tomato/wt}$, *Sox1*$^{Cre/wt}$;*Rosa26*$^{Tomato/wt}$, and

Pmx1-Cre$^{Tg/0}$;*Rosa26*$^{Tomato/wt}$ embryos.

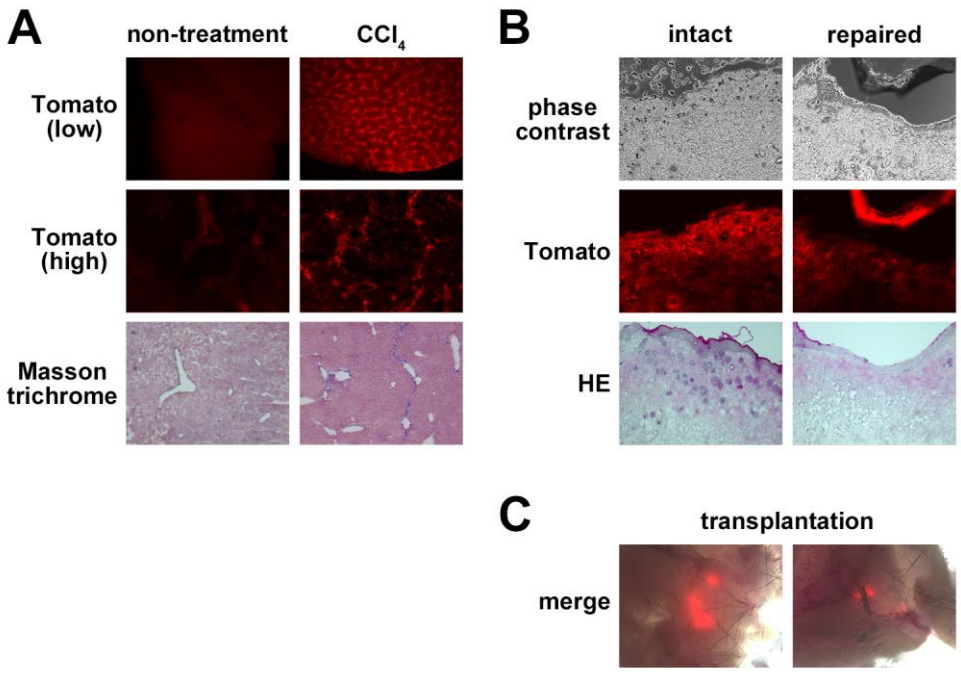

Fig. S5.

(A) Liver fibrosis in 15w *Pdgfra*$^{GCE/wt}$;*Rosa26*$^{Tomato/wt}$ mouse. The mouse was treated with 4-OHT at 8w and administrated routinely with carbon tetrachloride from 9w.

(B) Skin ulceration in 10w *Pdgfra*$^{GCE/wt}$;*Rosa26*$^{Tomato/wt}$ mouse. The mouse was treated with 4-OHT at 8w and underwent surgery at 9w.

(C) Skin ulceration in 8w mouse transplanted with Tomato-positive BM-MSC.

Table S1. Primers for RT-PCR

gene	sequence (forward)	sequence (reverse)
ß-Actin	5'-CCCTAAGGCCAACCGTGAAAAG-3'	5'-AGAGCATAGCCCTCGTAGATGG-3'
Gapdh	5'-ATGGTGAAGGTCGGTGTGAACG-3'	5'-TGCCGTGAGTGGAGTCATACTG-3'
Pdgfra	5'-CTTTCTGGTCCTCAGCTGTCTC-3'	5'-GGGTCGTCTTCTTCAGACATGG-3'
Brachyury	5'-ACCCAGACTCGCCCAATTTTGG-3'	5'-CTCTCACGATGTGAATCCGAGG-3'
Sox1	5'-ATGATGATGGAGACCGACCTGC-3'	5'-CACACCATGAAGGCGTTCATGG-3'
Pmx1	5'-GGCACAAGCAGACGAAAGTGTG-3'	5'-GTCCTGTTTCTCCGCTGCTTTC-3'
Pdgfrß	5'-ATGGGGCTTCCAGGAGTGATAC-3'	5'-CGAGCAGGTCAGAACAAAGGTG-3'
Sca1	5'-TTCTTGTGGCCCTACTGTGTGC-3'	5'-CCACAATAACTGCTGCCTCCTG-3'
CD51	5'-GGAAGTTACTTCGGATTCGCCG-3'	5'-TCAAACTCAATGGGCTGGCACC-3'
CD45	5'-GGAGACCCTATTTCTTAGGGGC-3'	5'-CCCAGAGTGGATGGTGTAAGAG-3'